Ann. Geophys., 30, 623–637, 2012
www.ann-geophys.net/30/623/2012/
doi:10.5194/angeo-30-623-2012

Annales Geophysicae

Multi-spacecraft observations of small-scale fluctuations in density and fields in plasmaspheric plumes

H. Matsui[1], F. Darrouzet[2], J. Goldstein[3], P. A. Puhl-Quinn[4], Yu. V. Khotyaintsev[5], P.-A. Lindqvist[6], E. Georgescu[7], C. G. Mouikis[1], and R. B. Torbert[1]

[1]Space Science Center, University of New Hampshire, 8 College Road, Durham, NH 03824, USA
[2]Belgian Institute for Space Aeronomy (IASB-BIRA), 3 Avenue Circulaire, 1180 Brussels, Belgium
[3]Southwest Research Institute, 6220 Culebra Road, San Antonio, TX 78228, USA
[4]AER, Inc., 131 Hartwell Ave., Lexington, MA 02421, USA
[5]Swedish Institute of Space Physics, Box 537, 751-21 Uppsala, Sweden
[6]Alfvén Laboratory, Royal Institute of Technology, 100-44 Stockholm, Sweden
[7]Max-Planck-Institut für Sonnensystemforschung, 37191 Katlenburg-Lindau, Germany

Correspondence to: H. Matsui (hiroshi.matsui@unh.edu)

Received: 27 August 2011 – Revised: 23 January 2012 – Accepted: 28 February 2012 – Published: 29 March 2012

Abstract. In this event study, small-scale fluctuations in plasmaspheric plumes with time scales of ∼10 s to minutes in the spacecraft frame are examined. In one event, plasmaspheric plumes are observed by Cluster, while IMAGE measured density enhancement at a similar location. Fluctuations in density exist in plumes as detected by Cluster and are accompanied by fluctuations in magnetic fields and electric fields. Magnetic fluctuations are transverse and along the direction of the plumes. The E/B ratio is smaller than the Alfvén velocity. Another similar event is briefly presented. We then consider physical properties of the fluctuations. Alfvén mode modulated by the feedback instability is one possibility, although non-local generation is likely. It is hard to show that the fluctuations represent a fast mode. Interchange motion is possible due to the consistency between measurements and expectations. The energy source could be a pressure or density gradient in plasmaspheric plumes. When more events are accumulated so that statistical analysis becomes feasible, this type of study will be useful to understand the time evolution of plumes.

Keywords. Magnetospheric physics (Plasmasphere)

1 Introduction

Plasmaspheric plumes are a salient feature of the near-Earth magnetosphere and have their origin in the plasmasphere (e.g., Lemaire and Gringauz, 1998; Goldstein, 2006; Darrouzet et al., 2008, 2009a,b). Formation of the plasmasphere itself was first explained by Nishida (1966) and Brice (1967). Basically, this is determined by an overlay of the convection and corotation electric fields. Subsequently, a plasmaspheric bulge is formed in the duskside (Carpenter, 1970). While the corotation electric field is essentially constant in time, the magnetospheric convection electric field changes continuously, which gives rise to the formation of a plasmaspheric tail (Taylor et al., 1968) or detached plasma elements (Chappell, 1974). These are now termed plasmaspheric plumes (Elphic et al., 1996; Goldstein et al., 2003). The plasmaspheric plume was successfully reproduced in previous simulation studies (Grebowsky, 1970; Chen and Wolf, 1972; Pierrard and Lemaire, 2004).

Density fluctuations in this spatial area, namely the main body of the plasmasphere and plumes, have been reported in previous articles. Higel (1978) examined GEOS 1 observations of density fluctuations with time scales varying between a few 10^{-1} s and 10 s (or spatial scales between a few 10^2 m and 10 km). CRRES (Combined Release and Radiation Effects Satellite) measured density fluctuations with a spectral power-law index of $-5/3$ (LeDocq et al., 1994). Density irregularities exist inside the plasmasphere measured by Cluster (Darrouzet et al., 2004). The small-scale density structures inside PBL (plasmasphere boundary layer) are one of the research topics discussed by Carpenter and Lemaire (2004). Goldstein et al. (2004) reported density fluctuations detected by LANL (Los Alamos National Laboratory)

geosynchronous satellites. Simultaneous observations of plumes are made by EUV (Extreme UltraViolet) instrument onboard IMAGE (Imager for Magnetopause-to-Aurora Global Exploration) satellite. Field aligned density structures have been reported by Carpenter et al. (2002). They used plasmagram data from IMAGE RPI (Radio Plasma Imager). McFadden et al. (2008) reported density fluctuations inside plumes measured by THEMIS (Time History of Events and their Macroscopic Interactions during Substorms) satellites. Borovsky and Denton (2008) examined density fluctuations and their relation to turbulence using LANL geosynchronous data.

Electromagnetic fluctuations are also reported in the same frequency range as the density fluctuations with periods ranging from seconds to minutes (e.g., McPherron, 2005). This frequency range corresponds to where Pc 1–5 waves are defined. Many of the fluctuations are identified as Alfvén waves propagating along magnetic field lines. When these waves propagate from the magnetosphere to the ionosphere, they are subsequently reflected. In some cases, a nonlinear effect, known as the feedback instability, takes place (Lysak and Song, 2002; Streltsov and Foster, 2004; Foster et al., 2004). Some of these Alfvén waves are mode-converted from fast mode waves which have their origin in the solar wind or at the magnetopause (Southwood, 1974; Chen and Hasegawa, 1974; Kivelson et al., 1984). As another possibility, the observed electromagnetic fluctuations are not waves, but the magnetospheric counterpart of static ionospheric currents (Gurnett et al., 1984; Dombeck et al., 2005) as studied in the auroral region. In this case, the ionospheric electric field is related to ionospheric currents through the Pedersen conductivity. Such electric fields are mapped to the magnetosphere in an electrostatic manner. Ionospheric currents would possibly be driven by the interchange motion of magnetic field lines (Richmond, 1973; Lemaire, 1974; Wolf, 1983; Ferrière et al., 1999). One energy source of the interchange motion is the pressure gradient in the magnetosphere. More specifically, when dealing with the plasmaspheric density structure, this could be the density gradient. The magnetospheric electric field mapped from the ionosphere could modify the shape of the locations with density gradient through the $\boldsymbol{E} \times \boldsymbol{B}$ drift and, hence, the interchange motion will grow or decay (Wolf, 1983). In a more rigorous treatment, the magnetohydrodynamic (MHD) wave modes are modified by the gravitational force, the gradient B/curvature drifts, etc. (Ferrière et al., 1999; Ferrière and André, 2003; André and Lemaire, 2006). Such a modified wave mode is called a quasi-interchange mode, although investigation on this mode is beyond the scope of this study. Here we concentrate on the interchange motion.

Cluster was launched in 2000 (Escoubet et al., 2001) and has various instruments with a capability to monitor plasmaspheric plumes. Four identical satellites with the same instrumentation could give spatio-temporal information. In addition, IMAGE was launched in the same year (Burch, 2000). These two missions are complementary because the Cluster satellites measure in situ quantities, while IMAGE satellite provides a global view. The objective of this study is to examine small-scale density fluctuations as well as accompanying electromagnetic fluctuations in plasmaspheric plumes using the Cluster unique dataset. We try to derive, from observations, a selection of possible physical properties of fluctuations. This type of study could advance our understanding of the spatio-temporal evolution of plumes.

The paper is organised as follows. We describe the dataset used in this study in Sect. 2. Then, we present one plume event with small-scale fluctuations in Sect. 3. The global context is provided by interplanetary and IMAGE data. Properties of fluctuations are examined in detail using multi-spacecraft, multi-instrument measurements made by Cluster. Another event is also briefly presented. We will discuss possible physical properties of fluctuations in Sect. 4. Here we consider Alfvén mode, fast mode and interchange motion. Future prospects are then described. Finally, the results are summarized in Sect. 5.

2 Dataset

We use mainly data from Cluster (Escoubet et al., 1997, 2001). The Cluster mission consists of four identical satellites (C1–C4). From its launch until 2006, each satellite follows a polar orbit with a perigee of 4 R_E and an apogee of 20 R_E. We pick events to analyse from this period. Cluster is equipped with various in situ instruments as described below. First we use number density data derived from the WHISPER (Waves of HIgh frequency and Sounders for Probing of Electron density by Relaxation) experiment (Décréau et al., 2001). The frequency range to detect electric field fluctuations is between 2 and 80 kHz. The electron plasma frequency in this range corresponds to density values lying between 0.05 and 80 cm^{-3}. Sounder data from which density is reliably determined are available every 52 s or 104 s. Passive data are used to derive additional density values. The sampling interval then decreases to 2 s at best. Here we use data with running averages of 10 s in order to reduce the effect of unrealistic density identification, which can occasionally happen. We also use spacecraft potential data measured by the double probes on EFW (Electric Field and Wave) instrument (Gustafsson et al., 2001). Good quality data at 4 s resolution are retrieved from Cluster Active Archive (Lindqvist et al., 2006; Khotyaintsev et al., 2010). This quantity is used as a proxy to number density. Three components of magnetic field data are recorded by FGM (FluxGate Magnetometer) (Balogh et al., 2001). 4 s spin period data are used in this study. There are two instruments measuring electric field onboard Cluster: the double probe instrument and electron drift instrument, both of which are used in this study. Two components of the electric field in the spacecraft spin plane are obtained by EFW double probes (Gustafsson et al., 2001).

The third component is calculated assuming no electric field parallel to the magnetic field when the magnetic field direction is more than 5 degrees from the spin plane. Good quality data at 4 s resolution are taken from Cluster Active Archive. We also sort out unrealistic data found by visual inspection. EFW data are suitable to investigate wave components as well as DC components. Here we analyse the AC components. In addition, two components of electric fields perpendicular to the ambient magnetic field are measured by EDI (Electron Drift Instrument) (Paschmann et al., 2001). The sampling interval is 1–4 s, although there are data gaps. We pick good quality data as in a previous study (Matsui et al., 2008). EDI data are suitable to investigate DC components. Electron count data with an energy of 1 keV with a pitch angle of 90 degrees are measured by EDI (Paschmann et al., 2001). These data are useful to identify the electron plasmasheet (Quinn et al., 2001). The sampling interval is 1 s. Density ratio of O^+/H^+ is estimated using data from RPA (Retarding Potential Analyzer) of CIS/CODIF (Cluster Ion Spectrometry/Composition Distribution Function Analyzer) (Rème et al., 2001).

We also use data from the IMAGE spacecraft (Burch, 2000). IMAGE has a polar orbit between 1000 and 45 600 km altitudes. There are various imaging instruments onboard. Here we analyse EUV images (Sandel et al., 2000). The EUV instrument takes images of resonant scatter of He^+ ions in EUV wavelength so that global views of the plumes are available. Data with a cadence of ∼10 min are made open to public.

Interplanetary data have been compiled as an OMNI database (King and Papitashvili, 2005). This database corrects nominal time lags of solar wind propagation between spacecraft locations, at which original data are measured, and the Earth's bow shock. We use 1 min resolution data for magnetic fields and plasmas. Concerning geomagnetic data, we introduce Dst and SYM-H indices in order to check for the occurrence of geomagnetic storms. The Dst index has a time resolution of 1 h, while SYM-H index has a higher resolution of 1 min. AU and AL indices with a resolution of 1 min are used to investigate substorm activities.

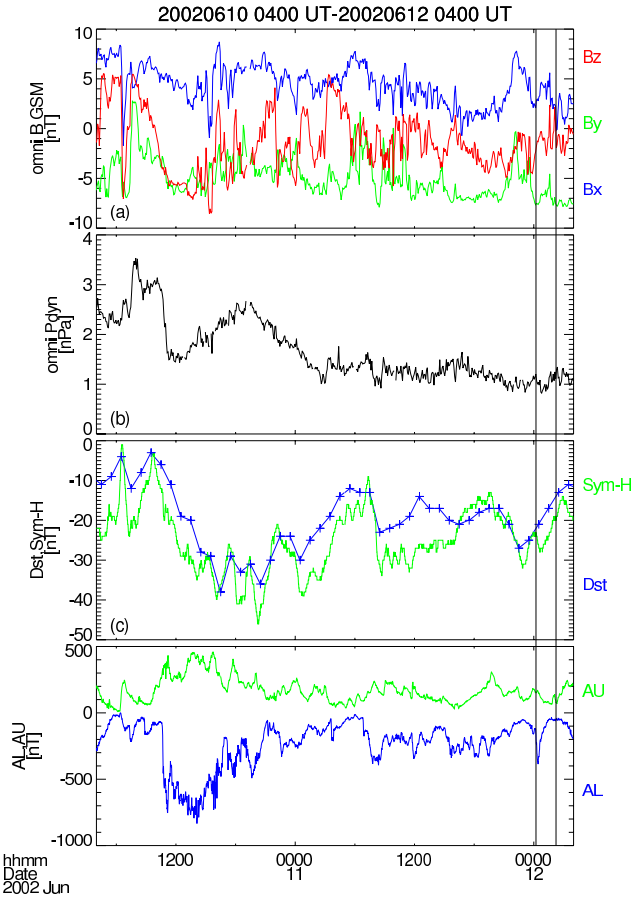

Fig. 1. Interplanetary and geomagnetic parameters from 04:00 UT on 10 June 2002 to 04:00 UT on 12 June 2002. From top to bottom: **(a)** The three components of IMF (interplanetary magnetic field) in GSM (geocentric solar-magnetospheric) coordinates from OMNI database, **(b)** the solar wind dynamic pressure from OMNI database, **(c)** Dst and SYM-H indices, and **(d)** AU and AL indices. Two vertical lines bracket the interval within which Cluster observed plumes.

3 Small-scale fluctuations in plumes

3.1 An event on 12 June 2002

Here we analyse one event of small-scale fluctuations in plasmaspheric plumes on 12 June 2002. Before showing the plume data, we first comment on interplanetary and geomagnetic conditions. Figure 1 shows interplanetary and geomagnetic parameters from 04:00 UT on 10 June 2002 to 04:00 UT on 12 June 2002. The two vertical guidelines bracket the intervals where Cluster observed plumes. IMF (interplanetary magnetic field) B_Z component in panel (a) is variable. It is often negative during the period with Cluster measurements and during the past 24 h. The dynamic pressure in panel (b) has a generally declining trend throughout the period from ∼3 nPa to ∼1 nPa. The Dst index in panel (c) shows a minimum at −38 nT at 16:00–17:00 UT on 10 June 2002, while SYM-H index in the same panel shows a similar trend. Then the values recover gradually. Therefore, the Cluster measurements are being performed during the recovery phase of a small geomagnetic storm. AU and AL indices in panel (d) show a persistent activity with a peak value reached around the same time of minimum Dst. The origin of the dynamical feature of the plume is considered a result of the IMF activity, especially the variability during the past 24 h. Continuously negative IMF B_Z lasting for hours would cause large magnetotail activity, which further enhances the ring current. The active geomagnetic conditions shown in this figure are favourable for plume occurrence (Burch et al., 2001).

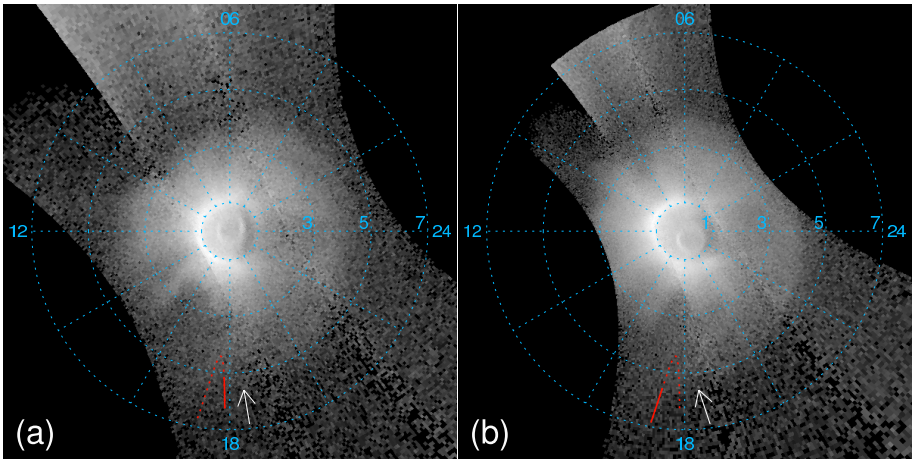

Fig. 2. Plasmaspheric images captured by IMAGE EUV and mapped to the magnetic equator on 12 June 2002 at **(a)** 00:18 UT and **(b)** 02:00 UT. Cluster (C1) orbital elements between 00:13 UT and 02:14 UT mapped to the equator along dipolar magnetic field lines are drawn by solid or dotted lines in red. The solid lines indicate Cluster orbital elements which correspond to plume crossings (00:13–00:35 UT and 01:57–02:14 UT) during when each image was taken, while the dotted lines indicate the rest of Cluster orbital elements. The view is from the northern pole. Leftside corresponds to noon MLT (magnetic local time). Selected L-values (1–7) and MLTs (06:00–24:00 MLT) are noted in the figure. Density is enhanced in the duskside as indicated by arrows.

Next we show plasmaspheric images captured by IMAGE EUV. Figure 2a and b shows those on 12 June 2002 at 00:18 and 02:00 UT, respectively. Images are mapped to the magnetic equator along dipole magnetic field lines assuming that the brightest points are located at innermost L-shells on the line-of-sight of each pixel (Roelof and Skinner, 2000). The view is from the northern pole. The leftside is toward the Sun. Cluster data are available when these images are taken. Cluster (C1) orbital elements during inbound and outbound plume crossings are indicated by red lines in panels (a) and (b), respectively. The solid lines indicate Cluster orbital elements which correspond to plume crossings during the time when each image was taken, while the dotted lines indicate the rest of Cluster orbital elements. These orbital elements are mapped to the equator along the dipole magnetic field lines. In both panels, the plasmasphere, which is considered as the origin of the plume, is observed. When we look at sequential images (figure not shown), the main motion is due to corotation. The plasmasphere does not have a teardrop shape, but includes density structures, one of which is a notch (Gallagher et al., 2005) located at $L \sim 3$ and ∼15:30–17:30 MLT (magnetic local time) in panel (a). This structure corotates to ∼17:00–18:00 MLT in panel (b). Density is enhanced in the duskside as indicated by an arrow in both panels. This is connected with the main body of the plasmasphere at $L \sim 4$ and ∼19:00 MLT and elongates toward $L \sim 6$ and ∼17:00 MLT. Cluster's orbits with plume measurements are close to the locations of this enhanced density in IMAGE data. Since the inner structure in the plasmaspheric images is not homogeneous, we expect irregularity in Cluster data, although the direct correspondence may not be clear due to the limited sensitivity of the EUV instrument, ∼40 cm^{-3} for protons (Goldstein et al., 2004), and the accuracy of the mapping procedure.

Figure 3 shows an overview of measurements made by C1 between 23:30 UT on 11 June 2002 and 02:50 UT on 12 June 2002. The spacecraft locations are noted in the bottom of the figure. The spacecraft was passing through the duskside perigee of 4.4 R_E at 01:38 UT. Density determined by WHISPER is shown in panel (a). The data gaps indicated by arrows are where the density lies above 80 cm^{-3}, which is the upper threshold of the instrument. Spacecraft potential measured by EFW in panel (b) is a proxy to density when there are gaps in density data (Pedersen et al., 2008). A larger spacecraft potential corresponds to larger density. There are two plume crossings. The first part is 00:13–00:35 UT, corresponding to the inbound plume crossing in the Southern Hemisphere. The second part is 01:57–02:14 UT, corresponding to the outbound plume crossing in the Northern Hemisphere. Plume intervals are indicated by pairs of vertical lines in Fig. 3. The spacecraft stayed in the inner plasmasphere between 00:35–01:06 UT and the plasma troughs during the rest of the time periods. Electron counts at an energy of 1 keV and a pitch angle of 90 degrees measured by EDI are shown in panel (c). Natural electron counts identified by the onboard calculation are selected from total counts which include both natural ones and artificial ones. The latter is used to determine the electric field. In addition, the counts are averages over 16 samples so that they could be less than 1. The large number of counts with a maximum of ∼100 counts in the beginning and the end of the plotted interval indicates that the spacecraft encountered the electron plasmasheet during those periods. The inner edge of the electron plasmasheet is measured at 23:50 and 02:33 UT.

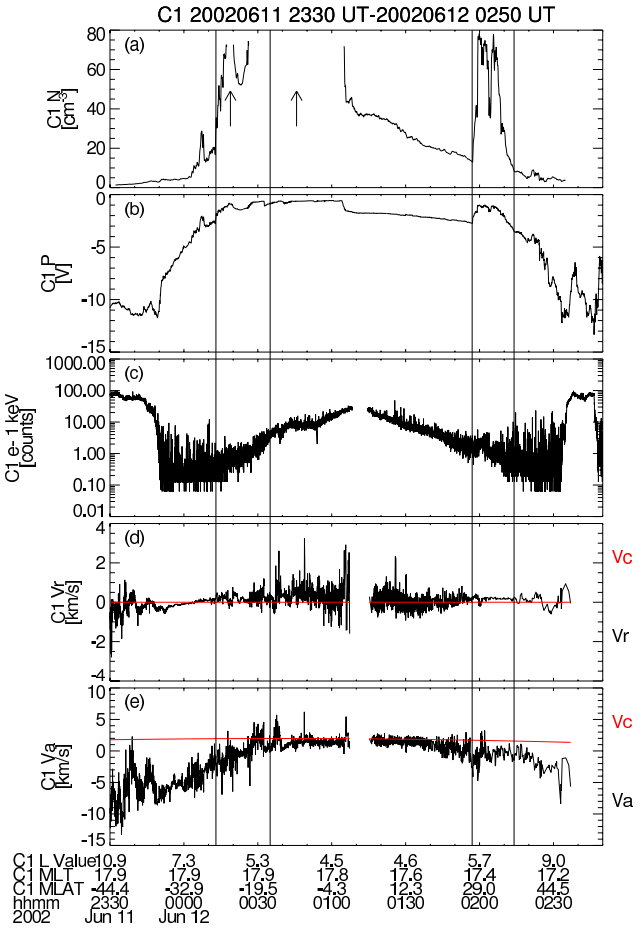

Fig. 3. C1 data including inbound and outbound plume crossings from 23:30 UT on 11 June 2002 to 02:50 UT on 12 June 2002. The figure shows **(a)** the number density, **(b)** spacecraft potential, **(c)** electron counts at 1 keV with a pitch angle of 90 degrees, and **(d)** radial and **(e)** azimuthal components of convection velocity together with corotation velocity. Spacecraft locations are noted in the bottom of the figure. Each plume crossing is indicated by pairs of vertical lines. Two arrows in panel **(a)** indicate data gaps caused by density values above 80 cm^{-3}, which is the upper threshold of the WHISPER instrument.

When we inspect the electron energy-time spectrogram from a particle instrument, the inner edges are inferred to be at 23:52 and 02:28 UT, similar to the EDI measurement, although there are data gaps for ∼2 h in between (figure not shown). The spacecraft was located in the sub-auroral region during the time interval inside the inner edges, which includes periods of both plume crossings. Panels (d) and (e) show the radial and azimuthal components of convection velocity measured by EDI, respectively. Positive values for each component indicate outward and eastward convection, respectively. The convection velocity is shown by black lines in the inertial frame, while the corotation velocity derived assuming a dipole field configuration is shown by red lines. The radial velocity is generally smaller than the azimuthal

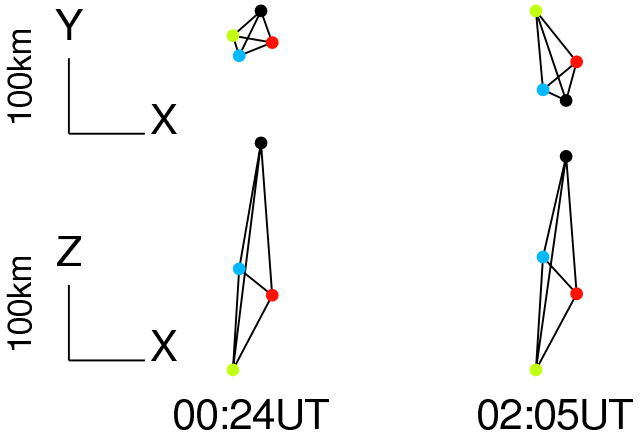

Fig. 4. Spacecraft constellations mapped to the X-Y and the X-Z planes in SM coordinates. The left and right part correspond to constellations during inbound and outbound plume crossings on 12 June 2002 at 00:24 UT and 02:05 UT, respectively. C1–4 are shown by black, red, green and blue, respectively.

velocity. The azimuthal velocity is close to the corotation velocity around the geomagnetic equator, while the negative value or westward component shows up away from the equator. Average westward velocity during the inbound and outbound plume crossings are 2.0 and 2.3 km s^{-1}, respectively, in the corotating frame. If we take into account the fact that each plume is located inside the sub-auroral region, the westward convection is considered as the sub-auroral polarization stream (SAPS) (e.g., Foster and Vo, 2002). There are small-scale fluctuations in density in plumes, which are examined more in detail below.

Figure 4 shows spacecraft constellations projected on the SM X-Y plane and the X-Z plane. The selected times at 00:24 and 02:05 UT are within the inbound and outbound plume crossings, respectively. The spacecraft separation is less than a few hundred km and elongated in the Z-direction.

Next we show fluctuations in density and electromagnetic fields measured by C1 from 00:00 to 02:20 UT on 12 June 2002 (Fig. 5). The density and spacecraft potential in panels (a) and (b), respectively, have already been introduced. Fluctuations in the density profile are shown in panel (c). These values are low-pass filtered twice by the second order Butterworth filter. There is no phase-shift between the original time-series and the filtered time-series. The corner period is set as 600 s. This type of filter was also adopted by Matsui et al. (2007). It should be noted that the filtered data are not plotted within 600 s from the data gap because the filter does not work so well during this interval. Fluctuations in density have a time scale of ∼10 s to minutes and the time-series are irregular. Fluctuations in magnetic fields from FGM and electric fields from EFW are shown in panels (d) and (e), respectively. Each quantity is plotted in field-aligned coordinates: parallel and two perpendicular components. The perpendicular components consist of radial and

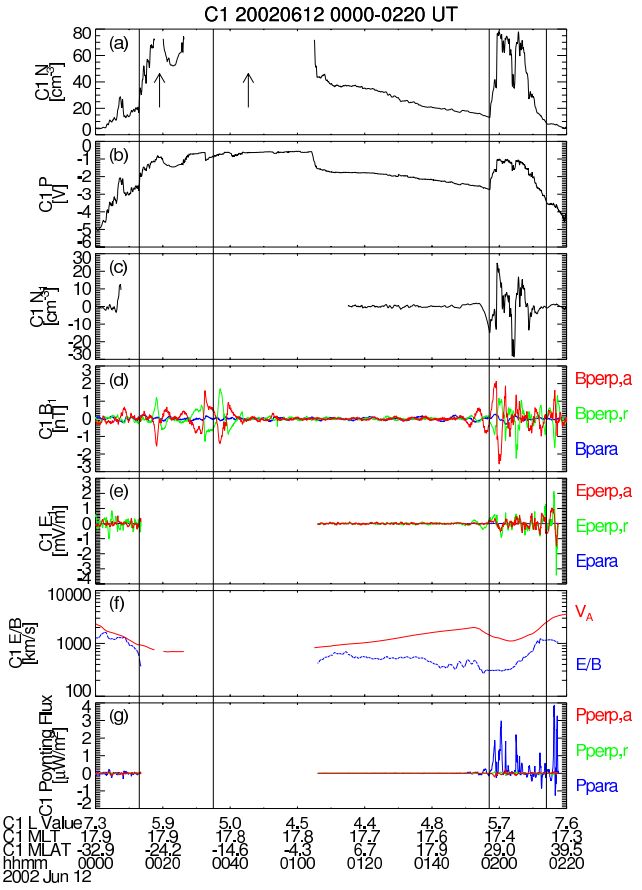

Fig. 5. C1 data including inbound and outbound plume crossings from 00:00 to 02:20 UT on 12 June 2002. The figure shows **(a)** the number density, **(b)** spacecraft potential, **(c)** density fluctuations, **(d)** magnetic fluctuations, **(e)** electric fluctuations, **(f)** E/B ratio together with the Alfvén velocity, and **(g)** Poynting flux. Spacecraft locations are noted in the bottom of the figure. Each plume crossing is indicated by pairs of vertical lines. Two arrows in panel **(a)** have the same meaning as those in Fig. 3.

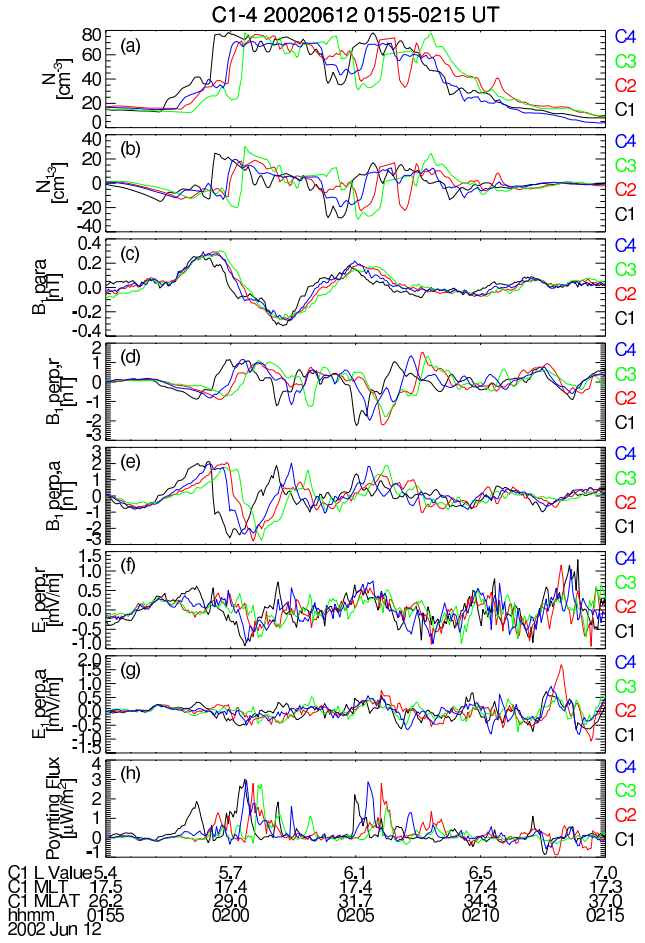

Fig. 6. Data from all Cluster spacecraft during the outbound plume crossing from 01:55 to 02:15 UT on 12 June 2002. The figure shows **(a)** the number density, **(b)** its fluctuations, **(c)**–**(e)** three components of magnetic fluctuations, **(f)**–**(g)** two perpendicular components of electric fluctuations, and **(h)** Poynting flux along the magnetic field. Spacecraft locations are noted in the bottom of the figure.

azimuthal components. These values are low-pass filtered in the same manner as the density values. When we inspect panels (d) and (e), we notice that fluctuations in magnetic fields and electric fields coexist when there are fluctuations in density. The density fluctuation is in the order of 10 cm^{-3}, while the magnetic fluctuation is $\sim$1 nT. The electric fluctuation is several tenths $\mathrm{mV\,m}^{-1}$ when the density fluctuation is seen. It should be noted that there is a data gap in the electric fluctuation especially during the inbound plume crossing. Magnetic fluctuations are mainly transverse to the magnetic field. Azimuthal components tend to be larger than radial ones. Taking into account the IMAGE observations, the orientation of main component is rather parallel to the direction in which the plume elongates, that is estimated to be outward and westward. Panel (f) shows the E/B ratio compared with the Alfvén velocity V_A. In order to get this ratio, we first calculate the sum of the three components of squared electric field fluctuations and those of the squared magnetic field fluctuations. Running averages of these two quantities are calculated with a sliding window of 600 s, and then the E/B ratio is derived. The wave components at various periods do not interfere with each other by averaging or integration because of the orthogonality of sinusoidal functions, if the integration period is long enough compared to the fluctuation period. In our case, the fluctuation period is between $\sim$10 s and several minutes. This averaging is useful to reduce fluctuations of E/B ratio shorter than the corner period, 600 s. Otherwise, the original ratio may take any values. As a simple example, if there are sinusoidal Alfvén waves, the averaging does not affect the estimate of the E/B ratio and even remove the singularity when the wave component changes its polarity. The Alfvén velocity is calculated using running averages of the magnetic field strength and density. We have

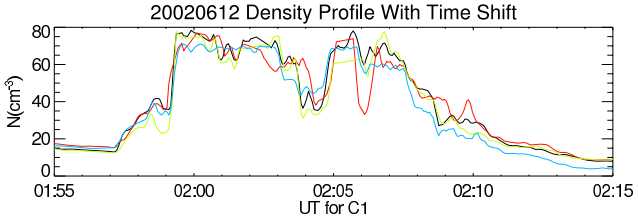

Fig. 7. Density profile during the outbound plume crossing between 01:55 and 02:15 UT on 12 June 2002. C2–4 data are shifted by −52, −72 and −36 s relative to C1 data, respectively. Meaning of each colour is the same as Fig. 4.

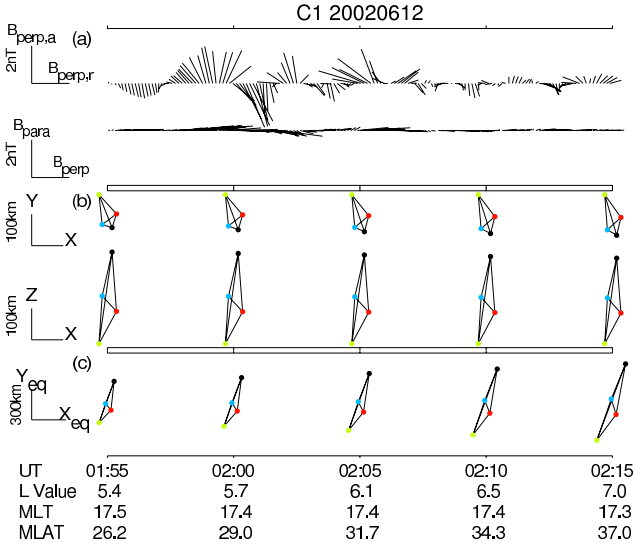

Fig. 8. Cluster data during the outbound plume crossing from 01:55 to 02:15 UT on 12 June 2002. The figure shows **(a)** magnetic fluctuations measured by C1 for two perpendicular components (radial and azimuthal components) in the top and magnetic fluctuations for perpendicular and parallel components in the bottom, **(b)** spacecraft constellation projected to the X-Y and the X-Z planes, and **(c)** spacecraft constellation mapped to the geomagnetic equator. In panel **(a)**, every one of two data points is plotted in order to increase visibility. In panels **(b)** and **(c)**, meaning of each colour is the same as Fig. 4. Spacecraft locations are noted in the bottom of the figure.

introduced a density ratio of O^+/H^+ of 3 % as the largest limit deduced from the CODIF instrument. Here we notice that the E/B ratio is less than the Alfvén velocity during the outbound plume crossing. Poynting flux in the parallel direction shown in panel (g) tends to be positive during the outbound plume crossing, indicating the energy flow toward the northern ionosphere in the same hemisphere. It is possible that the energy source is located in the magnetosphere, although we cannot deny the possibility that the energy propagates from the ionosphere in the Southern Hemisphere.

Figure 6 shows data from all four Cluster satellites during the outbound plume crossing at 01:55–02:15 UT, 12 June 2002. Quantities plotted are (a) density, (b) density fluctuations, (c)–(e) magnetic fluctuations, (f)–(g) electric fluctuations, and (h) Poynting flux in the parallel direction. Fluctuations are detected in all perpendicular components and by all spacecraft. Fluctuations between different spacecraft are similar but are not overlaid because of time lags within a few min. The similar density profiles between the four spacecraft have been confirmed by shifting the data by proper time lags (Fig. 7). Here the lags are determined so that the time-series between two spacecraft are best correlated. A time window to calculate each correlation is taken as 10 min and we have chosen median values of lags between 01:55 and 02:15 UT. In the original time series in Fig. 6, variations in time profiles in each quantity are first observed by C1, and then C4, C2 and C3 in this order. Taking into account the spacecraft constellation plotted in Fig. 4 and Fig. 8b, the variations are propagating toward the −Z direction in the spacecraft frame. This inference can be confirmed by the following calculation. Combining the estimated time lags with spacecraft separations (Décréau et al., 2005), we calculate the direction of the density gradient as (0.22, −0.18, −0.96) in SM coordinates or (0.07, −0.97, −0.24) in field-aligned coordinates. In the latter system, quantities shown are the parallel and the two perpendicular, radial and azimuthal, components in this order. The moving speed of the density structure along the normal is 3.3 km s^{-1} in the inertial frame. One component of the spacecraft motion in the same direction is estimated as −3.4 km s^{-1}, which is mostly the same in size, but in the opposite direction. Therefore, the propagation velocity of this fluctuation is consistent with orbital motion of the spacecraft. The fluctuation is considered as a static structure at the presented time-scales.

The orientation of the magnetic fluctuations is investigated in more detail in Fig. 8a. The result is shown in field-aligned coordinates for C1. Every one of two data points is plotted in order to increase visibility. As already explained, azimuthal components tend to be larger than radial components. There are actually 180 data points with azimuthal components larger than radial components, while there are 120 data points where the reverse is true. The ratio of average power of azimuthal components to that of radial components is calculated as 2.2. Parallel components are smaller than perpendicular components. Panel (b) shows the spacecraft constellation at the in situ spacecraft locations, which does not change much during the plotted interval. Panel (c) shows the same quantity mapped to the geomagnetic equator. Taking into account the spacecraft location in the evening sector, C1 and C3 are located at the largest and smallest L-values, respectively. Since the spacecraft is moving toward a larger L-shell, the constellation is consistent with the above inference that the spacecraft is observing a static structure.

The detailed feature of the fluctuations can be seen in frequency-time spectra of magnetic fields and electric fields (Fig. 9). The fluctuation is wideband in frequency between

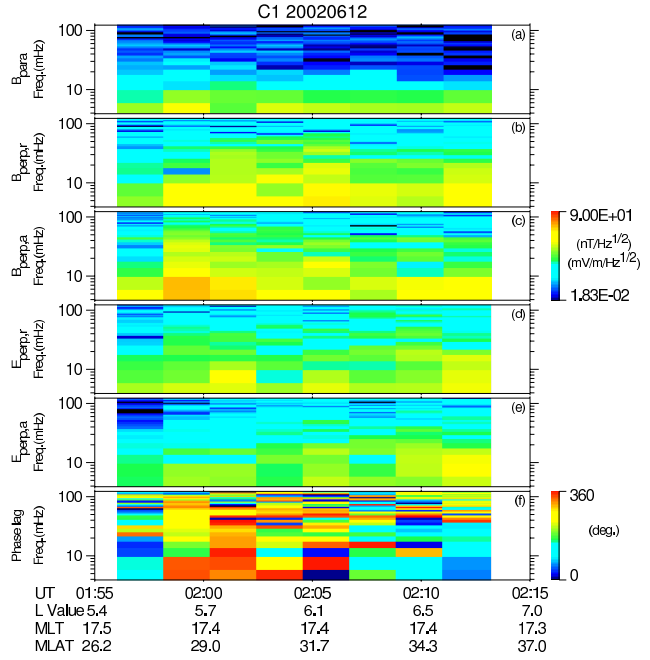

Fig. 9. Frequency-time spectra calculated using C1 data between 01:55 and 02:15 UT on 12 June 2002. Each panel shows **(a)**–**(c)** magnetic field spectra for three components, **(d)**–**(e)** electric field spectra for two perpendicular components and **(f)** phase lag between radial magnetic fluctuations and azimuthal electric fluctuations. Spacecraft locations are noted in the bottom of the figure.

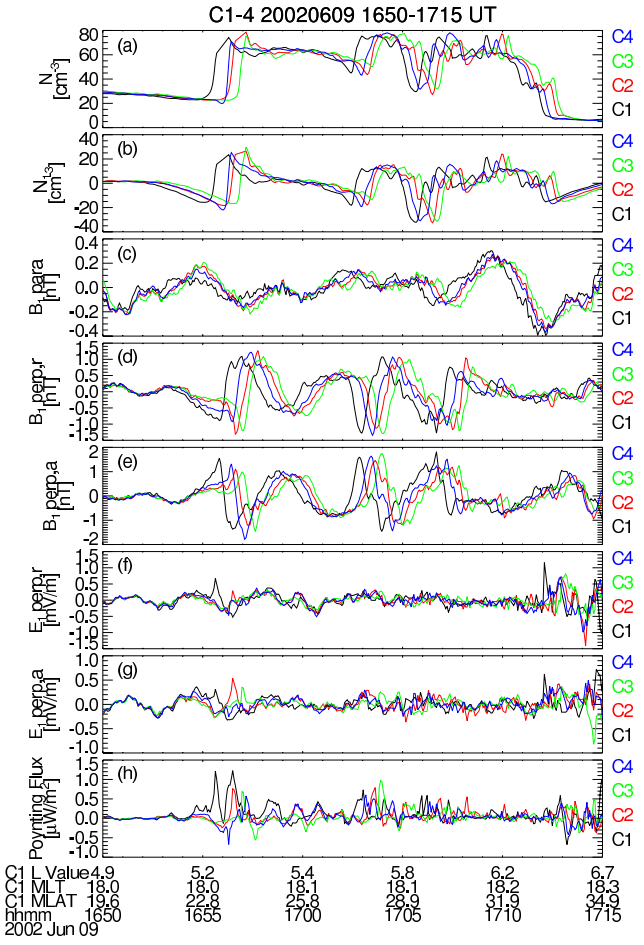

Fig. 10. Cluster data from all spacecraft during a plume crossing from 16:50 to 17:15 UT on 9 June 2002. Each panel shows the same quantity as Fig. 6.

several mHz and several tens mHz. The radial components tend to be smaller than the azimuthal components for the magnetic fluctuations, while the reverse is true for the electric fluctuations. The parallel components are smaller than perpendicular components for magnetic fluctuations. The bottom panel shows the phase lag between azimuthal components of the magnetic fluctuations and the radial components of electric fluctuations, both of which are the main components of the fluctuations. The phase lag is often close to 0 or 360 degrees at the lowest frequency end between 01:58 and 02:07 UT, where the wave power tends to increase. Therefore, we measure the total Poynting flux in the parallel direction in the same interval in Fig. 6h.

3.2 An event on 9 June 2002

We discuss briefly another event which occurred between 16:50–17:15 UT on 9 June 2002 (Fig. 10). This event has features similar to those of the previous event (figures not shown). Thus, there is IMF variability in the past 24 h. This event was again measured during the recovery of the Dst index with moderate AU/AL activity. IMAGE and Cluster measurements are consistent with each other. The Cluster spacecraft was located inside the inner edge of the electron plasmasheet. In Fig. 10 there are density enhancements corresponding to a plume. Small-scale fluctuations in density with a period of minutes or shorter are accompanied by fluctuations in the magnetic and electric fields. Fluctuations are similar to each other at all spacecraft which is confirmed by properly shifting the time-series (Fig. 11). Variations in time-series are first measured by C1 and then C4, C2, and C3 in this order. Taking into account the spacecraft constellation shown in Fig. 12b, the fluctuations seem to propagate toward the $-Z$ direction. In this case the normal direction of the density gradient is estimated as (0.74, −0.11, −0.66) in SM coordinates and (−0.06, −0.67, −0.74) in field-aligned coordinates. The density structure is moving at 3.5 km s^{-1} in this direction. The component of the spacecraft motion in the same direction is −3.8 km s^{-1}, similar to the above value but of opposite sign. The time-series from multiple spacecraft are again consistent with the spacecraft traversal of a static structure.

Figure 12a shows the orientation of the magnetic fluctuations for C1. Azimuthal components again tend to be larger than radial components. There are 249 such data points

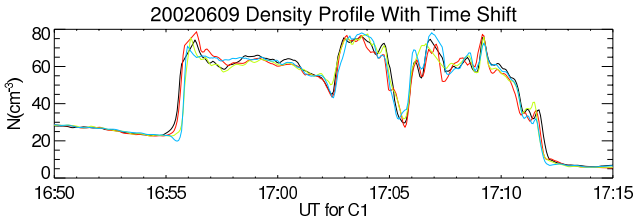

Fig. 11. Density profile during a plume crossing between 16:50 and 17:15 UT on 9 June 2002. C2–4 data are shifted by −48, −64 and −28 s relative to C1 data, respectively. The colour scheme is the same as in Fig. 4.

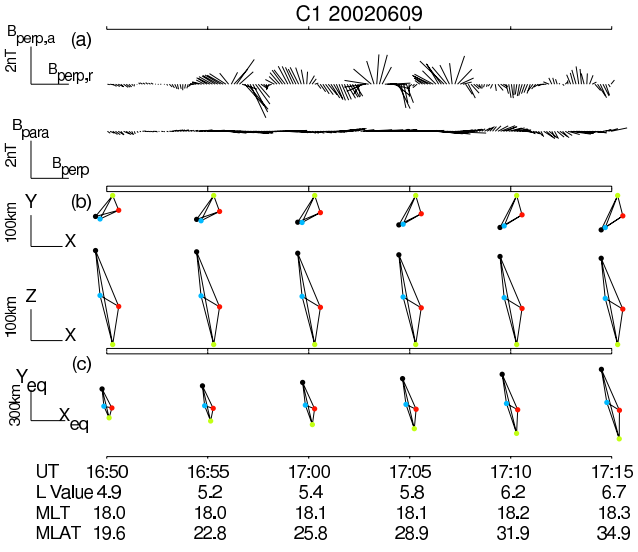

Fig. 12. Cluster data during a plume crossing from 16:50 to 17:15 UT on 9 June 2002. Each panel shows the same quantity as Fig. 8.

during the analysed interval, while there are 126 data points with azimuthal components smaller than radial components. The ratio of the average power of the azimuthal components to that of radial components is calculated as 1.8. Parallel fluctuations are generally smaller than perpendicular fluctuations. The spacecraft constellation at the in situ spacecraft location is shown in panel (b), which does not change much during the plotted interval. Panel (c) shows the spacecraft constellation mapped to the geomagnetic equator. C1 and C3 are again located at outermost and innermost L-shells, respectively. Taking into account spacecraft motion toward larger L-values, the temporal order of measured time-series is consistent with a static structure being sampled by the spacecraft.

Details of the fluctuations can be seen in frequency-time spectra (Fig. 13). Azimuthal fluctuations tend to be larger than radial fluctuations for magnetic fields, while the reverse is true for electric fields. Parallel components are smaller than perpendicular components for magnetic fluctuations.

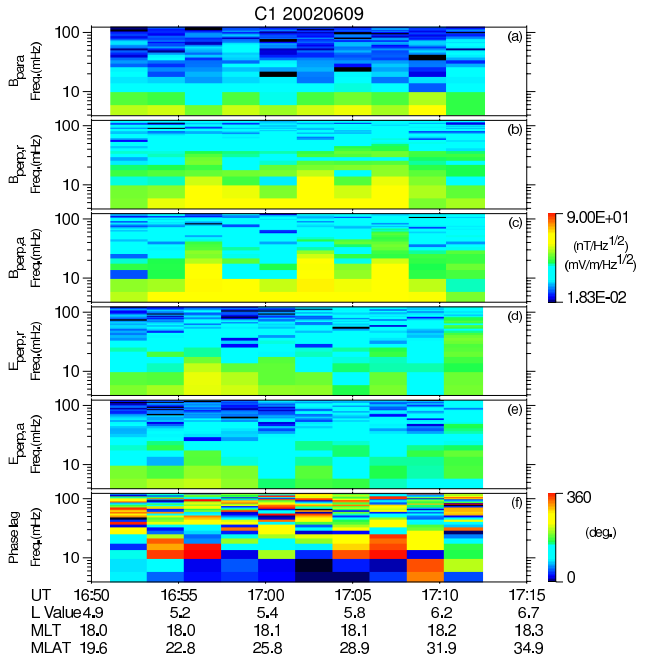

Fig. 13. Frequency-time spectra calculated using C1 data between 16:50 and 17:15 UT on 9 June 2002. Each panel shows the same quantity as Fig. 9.

Phase lag is shown between azimuthal magnetic fluctuations and radial electric fluctuations, which are the main component of fluctuations. The phase lag is close to 0 or 360 degrees around the lowest frequency end where the wave power increases. Therefore, the wave energy propagates along the magnetic field, as is also shown in Fig. 10h.

4 Discussion

We have analysed in detail one event of a plasmaspheric plume observed during the recovery of the Dst index. SAPS was measured during the plume crossings. We have observed fluctuations in density, magnetic field and electric field. A similar observation was made on another orbit. Here we try to discuss the physical properties of the fluctuations. We also discuss at the end future prospects of this study.

4.1 Possible physical properties of the fluctuations

There are various possible origins for these fluctuations: Alfvén mode, fast mode and interchange motion. Each possibility has the following characteristics. The Alfvén mode is commonly measured in the inner magnetosphere. The source of the fast mode is often regarded as the solar-wind magnetosphere coupling. Interchange motion is caused by plasma drift in the magnetosphere. M-I (Magnetosphere-ionosphere) coupling is essential. Below we consider each possibility more in detail.

4.1.1 Alfvén mode

Concerning the Alfvén mode, density fluctuations are usually not expected. However, these could exist when the feedback instability takes place at the ionospheric heights (e.g., Lysak and Song, 2002; Streltsov and Foster, 2004; Foster et al., 2004). Streltsov and Foster (2004) and Foster et al. (2004) reported this instability inside the SAPS region, which were also present in our events. Incoming Alfvén waves from the magnetosphere together with electron precipitation modify the ionospheric density. This instability is effective with low ionospheric conductivity, namely, at the nightside local times, and with large amplitude of incoming fluctuations. The latter condition is effective in becoming nonlinear and could be satisfied in our case depending on the mapping factor of the amplitude of fluctuations between the magnetosphere and the ionosphere and, hence, depending on density structure along the magnetic field line. Although our measurement is not really performed on the nightside, it is still possible that this instability takes place non-locally. The waves generated by this instability might convect from the nightside to the eveningside, where the spacecraft were located. The density structure generated by this mechanism could then become a seed for the interchange motion examined below. It should be noted, however, that this instability does not modify magnetospheric density directly. It is not clear to what degree or how quickly the magnetospheric density follows ionospheric one. As another possibility, density fluctuations might coincidentally exist with magnetic fluctuations, for example, because of spatial inhomogeneity of refilling.

In our observations, the E/B ratio is lower than the Alfvén speed, which seems inconsistent with this mode. However, if the waves are standing or reflected at the ionosphere, the ratio may take any values. Nonetheless, this idea is not so well supported when there is Poynting flux along the magnetic field lines as in our example because the pure standing mode implies that there is 90 degree phase shift between electric fluctuations and magnetic fluctuations.

4.1.2 Fast mode

The fast mode is considered unlikely for the following two reasons. (1) There are time lags of $\sim$10 s to min between magnetic fluctuations measured by different spacecraft. Referring to the spacecraft separations and the Alfvén velocity, such a lag for the fast mode is $<$0.5 s which is smaller than the time resolution of the present data analysis (4 s). Here we assume that the spatial scale of the fluctuations is longer than the spacecraft separation. We do not expect coherent time-series between different spacecraft if the spatial scale of the fluctuations is smaller than the spacecraft separation. (2) If we specify an amplitude of density fluctuations, that of the magnetic fluctuations can be estimated. The measured value is too small compared to the estimated value, if the temperature combining plasmaspheric and ring current materials is less than $\sim$10 keV or, in other words, the sound speed is smaller than the Alfvén speed. An example of such calculations is performed as follows referring to solutions of the MHD wave equations (e.g., McPherron, 2005). We choose the following parameters: background magnetic field of 500 nT, density of 60 cm^{-3}, amplitude of density fluctuation of 20 cm^{-3}. As long as the above condition for temperature $<\sim$10 keV is satisfied, the magnetic fluctuations are getting larger than 170 nT, which is much larger than the measured value of a few nT at most.

4.1.3 Interchange motion

Finally, we consider the possibility of interchange motion. If the fluctuation measured is related to a static ionospheric current, the E/B ratio mapped from the spacecraft location to the ionospheric height coincides with $1/\mu_0\Sigma_\mathrm{p}$, where μ_0 is the magnetic permeability in vacuum and Σ_p is the height-integrated Pedersen conductivity in the ionosphere (e.g., Gurnett et al., 1984). Here the magnetic fluctuation is assumed to be caused by field-aligned currents. If the fluctuation is in the Alfvén mode and is propagating as an alternative possibility, the E/B ratio coincides with the Alfvén velocity. Since the E/B ratio is smaller than the Alfvén velocity, it is possible that the fluctuation is caused by the ionospheric current.

Our next question concerns the origin of this current. If the energy source is located in the magnetosphere, the origin could be spontaneously induced diamagnetic currents flowing perpendicular to the pressure gradient, which is seen as the density gradient in our plots. Such spontaneously induced currents may be related to the interchange motion (e.g., Southwood and Kivelson, 1989). The possibility of the interchange motion around the plasmasphere has been suggested in several articles (Lemaire, 1974; Southwood et al., 2001; Carpenter et al., 2002; McFadden et al., 2008). The interchange motion has also been reported at outer planets (e.g., Kivelson et al., 1997; André et al., 2007).

The pressure gradient current could form a current system connected between the magnetosphere and the ionosphere. Figure 14 shows one possibility of such a current system. If there is pressure gradient perpendicular to the gradient of magnetic flux tube volume, field-aligned currents are generated (Vasyliūnas, 1970; Southwood and Kivelson, 1989). Since the gradient of the flux tube volume of the geomagnetic field is mainly in the radial direction, the azimuthal component of the pressure gradient is related to the field-aligned current. In our case, the direction of the pressure gradient or the density gradient is partly in the azimuthal direction even though the main component is radial for the event on 12 June 2002. Field-aligned currents thus generated are closed by an ionospheric current, which is related to the ionospheric electric field through the Pedersen conductivity. This electric field is mapped to the magnetosphere in an electrostatic manner. This scenario is consistent with the

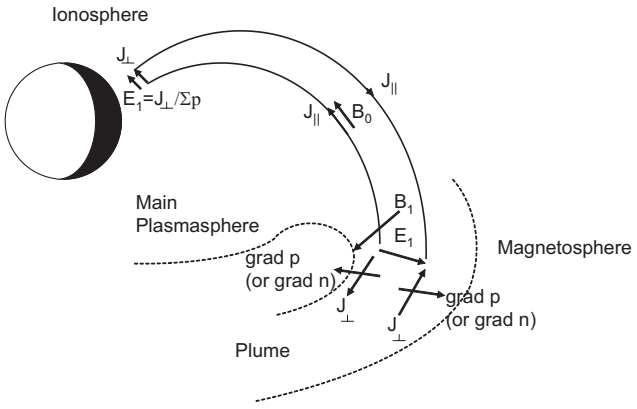

Fig. 14. One possible configuration of current system connecting the magnetosphere to the ionosphere. The current source is assumed to be a pressure gradient in the magnetosphere.

observation that density, magnetic and electric fluctuations are often concurrent.

Next we consider a simplified configuration where the radial component of the pressure gradient current is connected with the Pedersen current in the same radial or latitudinal direction, but with an opposite sign as depicted in the figure. The azimuthal magnetic fluctuation is expected when the field-aligned current is elongating or fairly homogeneous in the same direction and is connected to the ionospheric current in the radial direction (Smiddy et al., 1980). This situation tends to be consistent with the measured fluctuation with azimuthal components larger than radial components. It should be noted that the magnetic fluctuations have some radial components. This could be due partly to the simplification from the actual situation of the current closure and partly to the fact that the gradient of the magnetic flux volume of the geomagnetic field is not really radial.

We can roughly compare measured amplitudes of electromagnetic fluctuations with those expected in the above configuration. We adopt the following values for each parameter. Azimuthal component of the density gradient is approximated as $20\,\mathrm{cm}^{-3}/0.05\,R_\mathrm{E}$ at $L = 6$ in agreement with our measurement. The following are assumptions. The temperature of plume material is taken as $T = 1\,\mathrm{eV}$. The width of magnetospheric current in the latitudinal dimension is $5\,R_\mathrm{E}$. Pedersen conductance Σ_p is set equal to 3 mho. We also assume that the field-aligned current is closed with the radial component of the diamagnetic current. Physical quantities are considered as homogeneous in the azimuthal direction. The geomagnetic field is approximated by a dipole field when physical quantities are mapped between the magnetosphere and the ionosphere. One reference concerning the mapping of the electric field is Mozer (1970). From his derivation, we can infer mapping factors of the velocity and the magnetic deflection caused by the field-aligned current as well. Using the above quantities, the density of the diamagnetic current $\nabla p/B = T\nabla n/B$ in the radial direction is estimated as $7.2 \times 10^{-11}\,\mathrm{A\,m}^{-2}$. After multiplying by the thickness of the current sheet in the latitudinal direction, the current density per unit equatorial azimuthal length is calculated as $2.3 \times 10^{-3}\,\mathrm{A\,m}^{-1}$. We assume the same amount of ionospheric current is flowing in both hemispheres. The mapped ionospheric current in the radial direction in one hemisphere is $1.7 \times 10^{-2}\,\mathrm{A\,m}^{-1}$. The magnetic field deflection in the ionosphere caused by the field-aligned current is estimated by Smiddy et al. (1980). Such deflection in the azimuthal direction is calculated as 21 nT. Since Ohm's law in the ionosphere is $J = \Sigma_\mathrm{p} E$, the ionospheric electric field in the radial direction is derived as $5.6\,\mathrm{mV\,m}^{-1}$. The spacecraft is located around 30 degrees of magnetic latitude. The electric and magnetic field fluctuations mapped to the spacecraft location are estimated as $0.4\,\mathrm{mV\,m}^{-1}$ and 2.2 nT, respectively. These values are not inconsistent with our measurement (Fig. 5). Here we only consider the effect of the pressure gradient drift. We also calculated contributions of gradient B/curvature drift, gravitational drift and drift due to centrifugal force. They are smaller than that of the pressure gradient drift.

Again it should be noted that the above calculation is simplified with many assumptions. For example, there may be gradient of the ionospheric conductivity or spatial inhomogeneity in the actual situation. More rigorous treatment of this problem is beyond the scope of this study.

The electric fluctuations of order $0.1\,\mathrm{mV\,m}^{-1}$ correspond to the velocity fluctuation with $1\,\mathrm{km\,s}^{-1}$ or $0.5\,R_\mathrm{E}\,\mathrm{h}^{-1}$. Multiple Cluster spacecraft measure time profiles retaining similar features at least for a few min, which is a time lag of measurement between different spacecraft. IMAGE observations show that the density structures evolve relatively slowly. These indications for slow time evolution of structures are consistent with the expectation that the time-scale of electrostatic M-I coupling should be longer than the transit time of Alfvén waves between the magnetosphere and the ionosphere (e.g., Vasyliūnas, 2008), which has the same order as the period of Pc 5 waves.

The following points should be noted concerning this mode identification. In our example, the presence of ring current particles with tens or hundreds keV might not affect the current closure generated by plasmaspheric particles suggested above. This is because drift directions of ring current particles are different from those of plasmaspheric particles. The field structure would hardly be modified by quick traversal of ring current particles compared to plasmaspheric particles. In addition, the variations of energetic particle counts and those of density or fields do not seem to be so clearly related, although we cannot completely rule out a possible relation because of various time profiles of energetic particle counts. A careful investigation is required for this topic, which is left as future work.

It should also be noted that the physical property is essentially the same between the interchange motion and the

Alfvén mode. For example, both phenomena are related to field-aligned currents. However, other characteristics such as generation mechanisms and time scales are not necessarily the same. Interchange motion evolves slowly so that M-I coupling is electrostatic, while M-I coupling of the Alfvén mode is generally electromagnetic. Therefore, we tried to make distinction between these two phenomena.

We can discuss further the time scales of fluctuations by continuing the analysis. When we compare the velocity of the density structure in the inertial frame and the drift velocity from EDI, the difference is within $0.2\,\mathrm{km\,s^{-1}}$ in the direction of the density gradient. When we refer to the standard deviation of the drift velocity inside the plume events ($>1.0\,\mathrm{km\,s^{-1}}$), the difference between both measurements is smaller than this quantity. Therefore, the density structures are consistent with their being frozen in a reference frame moving with the drift velocity. Time lags estimated from the transverse components of the magnetic fluctuations tend to match those estimated from density fluctuations. In particular, the difference between time lags for azimuthal magnetic fluctuations and those for density fluctuations are within 4 s, which is the time resolution of the present analysis. Concerning the event on 9 June 2002, differences between time lags for radial magnetic fluctuations and those for density fluctuations are within 4 s as well. Therefore, the velocity of the magnetic structure tends to match that of density structure. Concerning electric fluctuation, the time lags often disagree with those of density and magnetic fluctuations possibly because electric fluctuations are more irregular than density and magnetic fluctuations as seen in Figs. 6 and 10. Correlation coefficients between lagged time series of electric fluctuations are generally smaller than those of magnetic and density fluctuations.

It is known that the interchange motion is accompanied by anticorrelation between density and magnetic field strength (e.g., Southwood et al., 2001). In our case, fluctuations in magnetic field strength caused by the pressure balance with fluctuations in density is $\sim$0.01 nT, which is too small to be detected. Here we have used typical parameters as follows: magnetic field strength of 500 nT, plasma temperature of 1 eV, and amplitude of density fluctuation of $20\,\mathrm{cm^{-3}}$.

The measured Poynting flux is directed toward the ionosphere. This looks consistent with the expectation that the energy source of this instability is located in the magnetosphere. However, this inference is not so conclusive because the wave energy might propagate from the ionosphere in another hemisphere. In addition, the direction of Poynting flux is variable when we checked another event.

4.2 Future prospects

Here we have presented case studies of fluctuations in plasmaspheric plumes. If, in future, we proceed to statistical analyses, we may obtain more constraints on the physical properties of the fluctuations. For example, the spatial distribution of the amplitudes of the fluctuations could give insight on the dependence of the fluctuations on the ionospheric conductivity because this quantity depends on local time. If magnetic fluctuations are often in the radial direction, our discussion on this quantity noted above becomes less ambiguous. In addition, frequency and wavelength provide further information to specify characteristics of fluctuations.

Theoretical work by Lemaire (1974) and Pierrard and Lemaire (2004) suggested that plume formation is caused by the interchange instability. If the fluctuations reported here are measured where plumes are actually generated, this may be relevant to their suggestions. Another aspect is the turbulent nature of plumes, examined by Borovsky and Denton (2008). Although our study does not focus on this feature, further study on this topic would advance our understanding of the time evolution of plumes.

5 Summary

In this work, we have studied fluctuations in plasmaspheric plumes through case studies. We have first examined one event on 12 June 2002, during which plumes are observed by Cluster. IMAGE data show density enhancements at a similar location. Fluctuations in plumes do not only exist in density but also in magnetic and electric fields. The magnetic fluctuation is mainly transverse and oriented along the plume direction. The E/B ratio is smaller than the Alfvén velocity. The time lag between multi-spacecraft time-series is consistent with spacecraft motion. We also have examined another event on 9 June 2002. Cluster and IMAGE observed similar features as the first event.

Based on the above observations, we have estimated possible physical properties of the fluctuations. One possibility is the Alfvén mode. If the waves are standing, the E/B ratio may take any values. Nonetheless, the Poynting flux along the magnetic field is measured, which is not expected for a pure standing mode. The standing mode implies that there is a 90 degree phase shift between electric fluctuations and magnetic fluctuations. There is a possibility that the density could be modulated by the feedback instability on the nightside and that the fluctuations are subsequently convected to the duskside. These waves might originally propagate from the magnetopause as the fast mode and then convert their mode to the Alfvén mode. The possibility of observing the fast mode itself is less likely. Another possibility is that the measured fluctuations are due to the interchange motion because of the following signatures: concurrent measurement of fluctuations in density, magnetic field and electric field; an estimated field variation consistent with the measurement; a E/B ratio lower than the Alfvén velocity; and relatively slow time evolution. The interchange motion is caused by the density gradient in plumes.

This type of study would be useful to understand the spatio-temporal evolution of fluctuations in plumes if we

identify more events in future. A larger database could be constructed using data from Cluster as well as coming RBSP (Radiation Belt Storm Probe).

Acknowledgements. Useful comments by K. Sigsbee during this work are acknowledged. Both reviewers' comments helped to improve the manuscript. C. J. Farrugia carefully read through the manuscript. EFW data are taken from Cluster Active Archive. We also browsed data provided by PEACE and RAPID teams on the same website. OMNI data were retrieved from NASA CDAweb. Dst, SYM-H, AU and AL indices were taken from the World Data Center at Kyoto University. This work was supported by NASA through a grant NNX07AI03G.

Guest Editor M. Taylor thanks P. M. E. Decreau and another anonymous referee for their help in evaluating this paper.

References

André, N. and Lemaire, J. F.: Convective instabilities in the plasmasphere, J. Atmos. Solar-Terr. Phys., 68, 213–227, 2006.

André, N., Persoon, A. M., Goldstein, J., Burch, J. L., Louarn, P., Lewis, G. R., Rymer, A. M., Coates, A. J., Kurth, W. S., Sittler Jr., E. C., Thomsen, M. F., Crary, F. J., Dougherty, M. K., Gurnett, D. A., and Young, D. T.: Magnetic signatures of plasma-depleted flux tubes in the Saturnian inner magnetosphere, Geophys. Res. Lett., 34, L14108, doi:10.1029/2007GL030374, 2007.

Balogh, A., Carr, C. M., Acuña, M. H., Dunlop, M. W., Beek, T. J., Brown, P., Fornacon, K.-H., Georgescu, E., Glassmeier, K.-H., Harris, J., Musmann, G., Oddy, T., and Schwingenschuh, K.: The Cluster Magnetic Field Investigation: overview of in-flight performance and initial results, Ann. Geophys., 19, 1207–1217, doi:10.5194/angeo-19-1207-2001, 2001.

Borovsky, J. E. and Denton, M. H.: A statistical look at plasmaspheric drainage plumes, J. Geophys. Res., 113, A09221, doi:10.1029/2007JA012994, 2008.

Brice, N. M.: Bulk Motion of the Magnetosphere, J. Geophys. Res., 72, 5193–5211, 1967.

Burch, J. L.: IMAGE mission overview, Space Sci. Rev., 91, 1–14, 2000.

Burch, J. L., Mitchell, D. G., Sandel, B. R., Brandt, P. C., and Wüest, M.: Global dynamics of the plasmasphere and ring current during magnetic storms, Geophys. Res. Lett., 28, 1159–1162, doi:10.1029/2000GL012413, 2001.

Carpenter, D. L.: Whistler evidence of the dynamic behavior of the duskside bulge in the plasmasphere, J . Geophys. Res., 75, 3837–3847, 1970.

Carpenter, D. L. and Lemaire, J.: The Plasmasphere Boundary Layer, Ann. Geophys., 22, 4291–4298, doi:10.5194/angeo-22-4291-2004, 2004.

Carpenter, D. L., Spasojević, M. A., Bell, T. F., Inan, U. S., Reinisch, B. W., Galkin, I. A., Benson, R. F., Green, J. L., Fung, S. F., and Boardsen, S. A.: Small-scale field-aligned plasmaspheric density structures inferred from the Radio Plasma Imager on IMAGE, J. Geophys. Res., 107, 1258, doi:10.1029/2001JA009199, 2002.

Chappell, C. R.: Detached plasma regions in the magnetosphere, J. Geophys. Res., 79, 1861–1870, 1974.

Chen, L. and Hasegawa, A.: A theory of long-period magnetic pulsations, 1. Steady state excitation of field line resonances, J. Geophys. Res., 79, 1024–1032, 1974.

Chen, A. J. and Wolf, R. A.: Effects on the plasmasphere of a time-varying convection electric field, Planet. Space Sci., 20, 483–509, 1972.

Darrouzet, F., Décréau, P. M. E., De Keyser, J., Masson, A., Gallagher, D. L., Santolik, O., Sandel, B. R., Trotignon, J. G., Rauch, J. L., Le Guirriec, E., Canu, P., Sedgemore, F., André, M., and Lemaire, J. F.: Density structures inside the plasmasphere: Cluster observations, Ann. Geophys., 22, 2577–2585, doi:10.5194/angeo-22-2577-2004, 2004.

Darrouzet, F., De Keyser, J., Décréau, P. M. E., El Lemdani-Mazouz, F., and Vallières, X.: Statistical analysis of plasmaspheric plumes with Cluster/WHISPER observations, Ann. Geophys., 26, 2403–2417, doi:10.5194/angeo-26-2403-2008, 2008.

Darrouzet, F., De Keyser, J., and Pierrard, V. (Eds.): The Earth's Plasmasphere: A CLUSTER and IMAGE Perspective, Springer, New York, 2009a.

Darrouzet, F., Gallagher, D. L., André, N., Carpenter, D. L., Dandouras, I., Décréau, P. M. E., De Keyser, J., Denton, R. E., Foster, J. C., Goldstein, J., Moldwin, M. B., Reinisch, B. W., Sandel, B. R., and Tu, J.: Plasmaspheric density structures and dynamics: Properties observed by the CLUSTER and IMAGE missions, Space Sci. Rev., 145, 55–106, 2009b.

Décréau, P. M. E., Fergeau, P., Krasnoselskikh, V., Le Guirriec, E., Lévêque, M., Martin, Ph., Randriamboarison, O., Rauch, J. L., Sené, F. X., Séran, H. C., Trotignon, J. G., Canu, P., Cornilleau, N., de Féraudy, H., Alleyne, H., Yearby, K., Mögensen, P. B., Gustafsson, G., André, M., Gurnett, D. C., Darrouzet, F., Lemaire, J., Harvey, C. C., Travnicek, P., and Whisper experimenters: Early results from the Whisper instrument on Cluster: an overview, Ann. Geophys., 19, 1241–1258, doi:10.5194/angeo-19-1241-2001, 2001.

Décréau, P. M. E., Le Guirriec, E., Rauch, J. L., Trotignon, J. G., Canu, P., Darrouzet, F., Lemaire, J., Masson, A., Sedgemore, F., and André, M.: Density irregularities in the plasmasphere boundary player: Cluster observations in the dusk sector, Adv. Space Res., 36, 1964–1969, 2005.

Dombeck, J., Cattell, C., Wygant, J. R., Keiling, A., and Scudder, J.: Alfvén waves and Poynting flux observed simultaneously by Polar and FAST in the plasma sheet boundary layer, J. Geophys. Res., 110, A12S90, doi:10.1029/2005JA011269, 2005.

Elphic, R. C., Weiss, L. A., Thomsen, M. F., McComas, D. J., and Moldwin, M. B.: Evolution of plasmaspheric ions at geosynchronous orbit during times of high geomagnetic activity, Geophys. Res. Lett., 23, 2189–2192, 1996.

Escoubet, C. P., Russell, C. T., and Schmidt, R. (Eds.): The Cluster and Phoenix Missions, Kluwer Academic Publishers, 1997.

Escoubet, C. P., Fehringer, M., and Goldstein, M.: Introduction: The Cluster mission, Ann. Geophys., 19, 1197–1200, doi:10.5194/angeo-19-1197-2001, 2001.

Ferrière, K. M. and André, N.: A mixed magnetohydrodynamic-kinetic theory of low-frequency waves and instabilities in stratified, gyrotropic, two-component plasmas, J. Geophys. Res., 108, 1308, doi:10.1029/2003JA009883, 2003.

Ferrière, K. M., Zimmer, C., and Blanc, M.: Magnetohydrodynamic waves and gravitational/centrifugal instability in rotating systems, J. Geophys. Res., 104, 17335–17356, 1999.

Foster, J. C. and Vo, H. B.: Average characteristics and activity dependence of the subauroral polarization stream, J. Geophys. Res., 107, 1475, doi:10.1029/2002JA009409, 2002.

Foster, J. C., Erickson, P. J., Lind, F. D., and Rideout, W.: Millstone Hill coherent-scatter radar observations of electric field variability in the sub-auroral polarization stream, Geophys. Res. Lett., 31, L21803, doi:10.1029/2004GL021271, 2004.

Gallagher, D. L., Adrian, M. L., and Liemohn, M. W.: Origin and evolution of deep plasmaspheric notches, J. Geophys. Res., 110, A09201, doi:10.1029/2004JA010906, 2005.

Goldstein, J.: Plasmasphere response: Tutorial and review of recent imaging results, Space Sci. Rev., 124, 203–216, 2006.

Goldstein, J., Sandel, B. R., Forrester, W. T., and Reiff, P. H.: IMF-driven plasmasphere erosion of 10 July 2000, Geophys. Res. Lett., 30, 1146, doi:10.1029/2002GL016478, 2003.

Goldstein, J., Sandel, B. R., Thomsen, M. F., Spasojević, M., and Reiff, P. H.: Simultaneous remote sensing and in situ observations of plasmaspheric drainage plumes, J. Geophys. Res., 109, A03202, doi:10.1029/2003JA010281, 2004.

Grebowsky, J. M.: Model study of plasmapause motion, J. Geophys. Res., 75, 4329–4333, 1970.

Gurnett, D. A., Huff, R. L., Menietti, J. D., Burch, J. L., Winningham, J. D., and Shawhan, S. D.: Correlated low-frequency electric and magnetic noise along the auroral field lines, J. Geophys. Res., 89, 8971–8985, 1984.

Gustafsson, G., André, M., Carozzi, T., Eriksson, A. I., Fälthammar, C.-G., Grard, R., Holmgren, G., Holtet, J. A., Ivchenko, N., Karlsson, T., Khotyaintsev, Y., Klimov, S., Laakso, H., Lindqvist, P.-A., Lybekk, B., Marklund, G., Mozer, F., Mursula, K., Pedersen, A., Popielawska, B., Savin, S., Stasiewicz, K., Tanskanen, P., Vaivads, A., and Wahlund, J.-E.: First results of electric field and density observations by Cluster EFW based on initial months of operation, Ann. Geophys., 19, 1219–1240, doi:10.5194/angeo-19-1219-2001, 2001.

Higel, B.: Small scale structure of magnetospheric electron density through on-line tracking of plasma resonances, Space Sci. Rev., 22, 611–631, 1978.

Khotyaintsev, Y., Lindqvist, P.-A., Eriksson, A. I., and André, M.: The EFW Data in the CAA, in: The Cluster Active Archive, Studying the Earth's Space Plasma Environment, edited by: Laakso, H., Taylor, M. G. T. T., and Escoubet, C. P., Astrophysics and Space Science Proceedings, pp. 97–108, Springer, Berlin, 2010.

King, J. H. and Papitashvili, N. E.: Solar wind spatial scales in and comparisons of hourly Wind and ACE plasma and magnetic field data, J. Geophys. Res., 110, A02104, doi:10.1029/2004JA010649, 2005.

Kivelson, M. G., Etcheto, J., and Trotignon, J. G.: Global compressional oscillations of the Terrestrial magnetosphere: The evidence and a model, J. Geophys. Res., 89, 9851–9856, 1984.

Kivelson, M. G., Khurana, K. K., Russell, C. T., and Walker, R. J.: Intermittent short-duration magnetic field anomalies in the Io torus: Evidence for plasma interchange?, Geophys. Res. Lett., 24, 2127–2130, 1997.

LeDocq, M. J., Gurnett, D. A., and Anderson, R. R.: Electron number density fluctuations near the plasmapause observed by the CRRES spacecraft, J. Geophys. Res., 99, 23661–23671, 1994.

Lemaire, J.: The 'Roche-limit' of ionospheric plasma and the formation of the plasmapause, Planet. Space Sci., 22, 757–766, 1974.

Lemaire, J. F. and Gringauz, K. I.: The Earth's Plasmasphere, Cambridge University Press, New York, 1998.

Lindqvist, P.-A., Khotyaintsev, Y., André, M., and Eriksson, A. I.: EFW data in the Cluster Active Archive, Proceedings Cluster and Double Star Symposium, ESA SP-598, 2006.

Lysak, R. L. and Song, Y.: Energetics of ionospheric feedback interaction, J. Geophys. Res., 107, 1160, doi:10.1029/2001JA000308, 2002.

Matsui, H., Puhl-Quinn, P. A., Torbert, R. B., Baumjohann, W., Farrugia, C. J., Mouikis, C. G., Lucek, E. A., Décréau, P. M. E., and Paschmann, G.: Cluster observations of broadband ULF waves near the dayside polar cap boundary: Two detailed multi-instrument event studies, J. Geophys. Res., 112, A07218, doi:10.1029/2007JA012251, 2007.

Matsui, H., Puhl-Quinn, P. A., Jordanova, V. K., Khotyaintsev, Y., Lindqvist, P.-A., and Torbert, R. B.: Derivation of inner magnetospheric electric field (UNH-IMEF) model using Cluster data set, Ann. Geophys., 26, 2887–2898, doi:10.5194/angeo-26-2887-2008, 2008.

McFadden, J. P., Carlson, C. W., Larson, D., Bonnell, J., Mozer, F. S., Angelopoulos, V., Glassmeier, K.-H., and Auster, U.: Structure of plasmaspheric plumes and their participation in magnetopause reconnection: First results from THEMIS, Geophys. Res. Lett., 35, L17S10, doi:10.1029/2008GL033677, 2008.

McPherron, R. L.: Magnetic pulsations: Their sources and relation to solar wind and geomagnetic activity, Surv. Geophys., 26, 545–592, 2005.

Mozer, F. S.: Electric field mapping in the ionosphere at the equatorial plane, Planet. Space Sci., 18, 259–263, 1970.

Nishida, A.: Formation of plasmapause, or magnetospheric plasma knee, by the combined action of magnetospheric convection and plasma escape from the tail, J. Geophys. Res., 71, 5669–5679, 1966.

Paschmann, G., Quinn, J. M., Torbert, R. B., Vaith, H., McIlwain, C. E., Haerendel, G., Bauer, O. H., Bauer, T., Baumjohann, W., Fillius, W., Förster, M., Frey, S., Georgescu, E., Kerr, S. S., Kletzing, C. A., Matsui, H., Puhl-Quinn, P., and Whipple, E. C.: The Electron Drift Instrument on Cluster: overview of first results, Ann. Geophys., 19, 1273–1288, doi:10.5194/angeo-19-1273-2001, 2001.

Pedersen, A., Lybekk, B., André, M., Eriksson, A., Masson, A., Mozer, F. S., Lindqvist, P.-A., Décréau, P. M. E., Dandouras, I., Sauvaud, J.-A., Fazakerley, A., Taylor, M., Paschmann, G., Svenes, K. R., Torkar, K., and Whipple, E.: Electron density estimations derived from spacecraft potential measurements on Cluster in tenuous plasma regions, J. Geophys. Res., 113, A07S33, doi:10.1029/2007JA012636, 2008.

Pierrard, V. and Lemaire, J. F.: Development of shoulders and plumes in the frame of the interchange instability mechanism for plasmapause formation, Geophys. Res. Lett., 31, L05809, doi:10.1029/2003GL018919, 2004.

Quinn, J. M., Paschmann, G., Torbert, R. B., Vaith, H., McIlwain, C. E., Haerendel, G., Bauer, O., Bauer, T. M., Baumjohann, W., Fillius, W., Foerster, M., Frey, S., Georgescu, E., Kerr, S. S., Kletzing, C. A., Matsui, H., Puhl-Quinn, P., and Whipple, E. C.: Cluster EDI convection measurements across the high-latitude plasma sheet boundary at midnight, Ann. Geophys., 19, 1669–

1681, doi:10.5194/angeo-19-1669-2001, 2001.

Rème, H., Aoustin, C., Bosqued, J. M., Dandouras, I., Lavraud, B., Sauvaud, J. A., Barthe, A., Bouyssou, J., Camus, Th., Coeur-Joly, O., Cros, A., Cuvilo, J., Ducay, F., Garbarowitz, Y., Medale, J. L., Penou, E., Perrier, H., Romefort, D., Rouzaud, J., Vallat, C., Alcaydé, D., Jacquey, C., Mazelle, C., d'Uston, C., Möbius, E., Kistler, L. M., Crocker, K., Granoff, M., Mouikis, C., Popecki, M., Vosbury, M., Klecker, B., Hovestadt, D., Kucharek, H., Kuenneth, E., Paschmann, G., Scholer, M., Sckopke, N., Seidenschwang, E., Carlson, C. W., Curtis, D. W., Ingraham, C., Lin, R. P., McFadden, J. P., Parks, G. K., Phan, T., Formisano, V., Amata, E., Bavassano-Cattaneo, M. B., Baldetti, P., Bruno, R., Chionchio, G., Di Lellis, A., Marcucci, M. F., Pallocchia, G., Korth, A., Daly, P. W., Graeve, B., Rosenbauer, H., Vasyliunas, V., McCarthy, M., Wilber, M., Eliasson, L., Lundin, R., Olsen, S., Shelley, E. G., Fuselier, S., Ghielmetti, A. G., Lennartsson, W., Escoubet, C. P., Balsiger, H., Friedel, R., Cao, J.-B., Kovrazhkin, R. A., Papamastorakis, I., Pellat, R., Scudder, J., and Sonnerup, B.: First multispacecraft ion measurements in and near the Earth's magnetosphere with the identical Cluster ion spectrometry (CIS) experiment, Ann. Geophys., 19, 1303–1354, doi:10.5194/angeo-19-1303-2001, 2001.

Richmond, A. D.: Self-induced motions of thermal plasma in the magnetosphere and the stability of the plasmapause, Radio Sci., 8, 1019–1027, 1973.

Roelof, E. C. and Skinner, A. J.: Extraction of ion distributions from magnetospheric ENA and EUV images, Space Sci. Rev., 91, 437–459, 2000.

Sandel, B. R., Broadfoot, A. L., Curtis, C. C., King, R. A., Stone, T. C., Hill, R. H., Chen, J., Siegmund, O. H. W., Raffanti, R., Allred, D. D., Turley, R. S., and Gallagher, D. L.: The extreme ultraviolet imager investigation for the IMAGE mission, Space Sci. Rev., 91, 197–242, 2000.

Smiddy, M., Burke, W. J., Kelley, M. C., Saflekos, N. A., Gussenhoven, M. S., Hardy, D. A., and Rich, F. J.: Effects of high-latitude conductivity on observed convection electric fields and Birkeland currents, J. Geophys. Res., 85, 6811–6818, 1980.

Southwood, D. J.: Some features of resonances in the magnetosphere, Planet. Space Sci., 22, 483–491, 1974.

Southwood, D. J. and Kivelson, M. G.: Magnetospheric interchange motions, J. Geophys. Res., 94, 299–308, 1989.

Southwood, D. J., Dougherty, M. K., Balogh, A., Cowley, S. W. H., Smith, E. J., Tsurutani, B. T., Russell, C. T., Siscoe, G. L., Erdos, G., Glassmeier, K.-H., Gleim, F., and Neubauer, F. M.: Magnetometer measurements from the Cassini Earth swing-by, J. Geophys. Res., 106, 30109–30128, 2001.

Streltsov, A. V. and Foster, J. C.: Electrodynamics of the magnetosphere-ionosphere coupling in the nightside subauroral zone, Phys. Plasmas, 11, 1260–1267, 2004.

Taylor, Jr., H. A., Brinton, H. C., and Pharo, III, M. W.: Contraction of the plasmasphere during geomagnetically disturbed periods, J. Geophys. Res., 73, 961–968, 1968.

Vasyliūnas, V. M.: Mathematical models of magnetospheric convection and its coupling to the ionosphere, in: Particles and Fields in the Magnetosphere, edited by: McCormac, B. M., pp. 60–71, D. Reidel, Dordrecht, The Netherlands, 1970.

Vasyliūnas, V. M.: Understanding the magnetosphere: The counter-intuitive simplicity of cosmic electrodynamics, Eos Trans. AGU, 89, Fall Meet. Suppl. Abstract SM33B-01, 2008.

Wolf, R. A.: The quasi-static (slow-flow) region of the magnetosphere, in: Solar-Terrestrial Physics, edited by: Carovillano, R. L. and Forbes, J. M., pp. 303–368, D. Reidel, Dordrecht, The Netherlands, 1983.